12. V. I. Alimpiev, A. L. Sorokin, and V. G. Safonov, Boundary Layers under Complex Conditions [in Russian], Novosibirsk (1984), pp. 5-15.
13. A. D. Gosmen, V. M. Pan, A. K. Ranchel, et al., Numerical Methods for Study of Viscous Liquid Flows [in Russian], Moscow (1972).
14. P. J. Roache, Computational Fluid Dynamics, Hermosa (1976).

CALCULATION OF NOZZLE FLOW WITH MIXING IN THE PRESENCE OF A STRONG VORTICITY EFFECT

V. I. Vasil'ev

UDC 532.522.2:519.633

A method of calculating the essentially three-dimensional turbulent flow in a mixing channel is proposed. The results of calculating the nozzle flow behind a mixer is presented.

1. In mixing nozzles, mixers generally of the tab type, are used to intensify the mixing process. The distribution of the parameters behind a mixer at the nozzle inlet is circumferentially nonuniform, and the flow is essentially three-dimensional. Experiments [1] have also shown that the flow over a curved mixer surface may create intense longitudinal vortices, under whose influence one of the streams separates into a number of jets.

The calculation of nozzle flows behind mixers was the subject of studies [2, 3]. In [2] the Patankar–Spalding method [4], intended for the numerical integration of the parabolized Navier–Stokes equations, was employed. The calculations were compared with the experimental data, but the lack of information on the cross flow fields at the mixer exit face made it impossible to obtain good agreement. In [3] the experimental data of [1] were used as the conditions at the mixer exit and the results of the calculations were found to be in satisfactory qualitative and quantitative agreement with experiment. These calculations made use of a method [5] originally developed for investigating flows in curved channels. The parameter distributions were found by numerical integration of the equations written in a coordinate system moving with the inviscid gas streamlines in a nozzle of the same geometry but without mixing. The pressure distribution was represented as the sum of the pressure fields in the inviscid gas flow and a correction for mixing. In this case the calculations are more complicated than when the method adopted in [2] is employed.

Our aim was to show that when the true nature of the cross flows at the mixer exit is taken into account, the parabolized Navier–Stokes equations make it possible to describe the mixing process in the nozzle. The cross flows are calculated using the approach proposed in [6], extended to the case of compressible gas flows. For describing the cross flows due to vorticity it is also proposed to employ simplified relations that are exact in the limiting case – the mixing of flows with only slightly different parameters.

2. The parabolized Navier–Stokes equations describe weakly expanding flows, i.e., flows in which the parameters in a preferred direction vary much more weakly than in the transverse section. For subsonic perfect gas flows with constant specific heats in the cylindrical coordinate system in which x is the axial coordinate in the preferred direction these equations take the form:

$$\frac{\partial \rho u^2}{\partial x} + \operatorname{div}(\rho \mathbf{V} u) = -\frac{dP}{dx} + \operatorname{div}(\rho \nu_t \nabla u), \tag{1}$$

$$\frac{\partial \rho u v}{\partial x} + \operatorname{div}(\rho \mathbf{V} v) = -\frac{\partial p}{\partial y} + \frac{1}{y}\frac{\partial}{\partial y}(y\tau_{yy}) + \frac{1}{y}\frac{\partial \tau_{y\theta}}{\partial \theta} - \frac{\tau_{\theta\theta}}{y}, \tag{2}$$

Translated from Inzhenerno-Fizicheskii Zhurnal, Vol. 54, No. 4, pp. 565-572, April, 1988. Original article submitted October 21, 1986.

0022-0841/88/5404-0385$12.50

$$\frac{\partial \rho u w}{\partial x} + \operatorname{div}(\rho \mathbf{V} w) = -\frac{1}{y}\frac{\partial p}{\partial \theta} + \frac{1}{y^2}\frac{\partial}{\partial y}(y^2 \tau_{y\theta}) + \frac{1}{y}\frac{\partial \tau_{\theta\theta}}{\partial \theta}, \tag{3}$$

where

$$\tau_{yy} = 2\rho \nu_t \frac{\partial v}{\partial y};\ \tau_{y\theta} = \rho \nu_t \left(\frac{1}{y}\frac{\partial v}{\partial \theta} + y\frac{\partial}{\partial y}\left(\frac{w}{y}\right)\right);$$

$$\tau_{\theta\theta} = 2\rho \nu_t \left(\frac{1}{y}\frac{\partial w}{\partial \theta} + \frac{v}{y}\right);$$

$$\frac{\partial \rho u T^*}{\partial x} + \operatorname{div}(\rho \mathbf{V} T^*) = 1/\mathrm{Pr}_t \operatorname{div}(\rho \nu_t \nabla T^*); \tag{4}$$

$$\frac{\partial \rho u}{\partial x} + \operatorname{div}(\rho \mathbf{V}) = 0; \tag{5}$$

$$\frac{\varkappa - 1}{\varkappa}\rho(c_p T^* - u^2/2) = P(x). \tag{6}$$

Here, the scalar operator $\operatorname{div} = \frac{1}{y}\frac{\partial}{\partial y}y + \frac{1}{y}\frac{\partial}{\partial \theta}$ and the vector operator ∇ with components $(\partial/\partial y,\ 1/y\frac{\partial}{\partial \theta})$ act in the transverse plane. The pressure is represented in the form of a sum of components: a component constant over the cross section P(x) and a variable component p(x, y, ϑ), and in a weakly expanding flow the longitudinal gradient of p in the equation of motion (1) can be disregarded (for an estimate see [6]). The components of the turbulent Reynolds stress tensor and the heat flux vector are expressed in terms of the mean velocity and temperature gradients by means of the Boussinesq hypothesis. For the turbulent Prandtl number, in accordance with [7], we took the value $\mathrm{Pr}_t = 0.8$; the specific heat ratio $\varkappa$ was set equal to 1.4. Since the flows considered are purely subsonic, in the energy equation (4) we have neglected the dissipative term, whose ratio to the diffusion term is equal to $\frac{\varkappa - 1}{2}(1 - 1/\mathrm{Pr}_t)\,M^2$, the corresponding correction not exceeding 5%.

The turbulent viscosity coefficient was determined using the one-parameter model [8]

$$\frac{\partial \rho u \nu_t}{\partial x} + \operatorname{div}(\rho \mathbf{V} \nu_t) = \operatorname{div}(2\rho \nu_t \nabla \nu_t) + 0{,}2\rho \nu_t |\nabla u|. \tag{7}$$

In (7) allowance has been made for the fact that in the mixing zones the laminar viscosity coefficient is much less than the turbulent one and hence can be disregarded.

In [6], in order to calculate the cross flows in cases where the longitudinal velocity component does not vanish (in the mixing zone this condition is satisfied), it was proposed that the following transformation of variables be employed:

$$v = \frac{\partial \varphi}{\partial y} + u/y\frac{\partial \psi}{\partial \theta};\ w = 1/y\frac{\partial \varphi}{\partial \theta} - u\frac{\partial \psi}{\partial y}. \tag{8}$$

The governing equations for the functions φ and ψ do not contain terms with the pressure field component p, and the method of calculating the transverse velocities is somewhat more efficient than that used in [4]. The equation for the secondary flow potential φ is obtained by substituting (8) in the compatibility condition. In its turn, the compatibility condition is obtained by eliminating the derivative $\partial \rho u/\partial x$ from the continuity equation (5) using the equations of state (6), energy (4) and motion (1). Differentiating (6), we obtain

$$\frac{\partial \rho}{\partial x} = \rho/P\frac{dP}{dx} - \frac{\varkappa - 1}{\varkappa}C_p \rho^2/P\frac{\partial T^*}{\partial x} + \frac{\varkappa - 1}{\varkappa}\frac{\rho^2 u}{P}\frac{\partial u}{\partial x}.$$

When the continuity equation is taken into account, relations (1) and (4) make it possible to express the derivatives $\partial u \partial x$ and $\partial T^*/\partial x$ as functions of the parameters in the section in question. Substituting these expressions in (5) instead of $\rho\frac{\partial u}{\partial x} + u\frac{\partial \rho}{\partial x}$, collecting like terms and, finally, using (8), we arrive at the final equation

$$\operatorname{div}(\nabla \varphi/u) = \frac{1 - M^2}{\rho u^2}\frac{dP}{dx} - \frac{1 + (\varkappa - 1)M^2}{\rho u^2}\operatorname{div}(\rho \nu_t \nabla u) + \frac{\varkappa - 1}{\varkappa}\frac{c_p}{uP}\frac{1}{\mathrm{Pr}_t}\operatorname{div}(\rho \nu_t \nabla T^*). \tag{9}$$

From the given distributions of u, ρ, and ν_t in the initial section and the value of P this relation also enables us to find the initial distribution of the secondary flow potential. From the condition of conservation of the flow rate in the channel it follows that the integral over the cross section on the right side of (9) is equal to zero; consequently, integrating the right side, we obtain a relation for determining the pressure gradient in the section in question.

In order to obtain an equation for the vortex component of the secondary flows, it is necessary to differentiate the expression (2) with respect to ϑ and (3) with respect to y and to subtract one from the other, thus eliminating p. Having made the substitution (8), we arrive at the relation

$$\operatorname{div}\left[\rho u\frac{\partial}{\partial x}(u\nabla\psi)\right]+\operatorname{div}\left[\rho\mathbf{V}\operatorname{div}(u\nabla\psi)\right]=\frac{1}{y}\left(\frac{\partial\rho u}{\partial y}\frac{\partial^2\varphi}{\partial x\partial\theta}-\right.$$

$$\left.-\frac{\partial\rho u}{\partial\theta}\frac{\partial^2\varphi}{\partial x\partial y}\right)+\frac{1}{y}\left(\frac{\partial\rho}{\partial y}\frac{\partial}{\partial\theta}\frac{|\mathbf{V}|^2}{2}-\frac{\partial\rho}{\partial\theta}\frac{\partial}{\partial y}\frac{|\mathbf{V}|^2}{2}\right)- \tag{10}$$

$$-\left[\frac{1}{y}\frac{\partial}{\partial y}\left(\frac{1}{y}\frac{\partial}{\partial y}y^2\tau_{y\theta}\right)-\frac{1}{y^2}\frac{\partial^2}{\partial\theta^2}\tau_{y\theta}\right]+\frac{1}{y}\frac{\partial}{\partial y}\left[y\frac{\partial}{\partial\theta}(\tau_{yy}-\tau_{\theta\theta})\right].$$

This fourth-order evolution equation serves for determining the function ψ (when the substitution (8) is made, the fourth derivatives of ψ with respect to the variables y and ϑ enter into the terms with τ; here, however, the right side has not been written out in its final form because of the clumsiness of the expressions). For this equation to be integrated numerically, it must be split into two second-order equations. By analogy with [6] this can be done by introducing the variable

$$\chi=\frac{1}{\rho uy}\left(\frac{\partial\rho uyw}{\partial y}-\frac{\partial\rho uv}{\partial\theta}\right). \tag{11}$$

Substituting (8) in (11), we obtain a two-dimensional elliptic equation for determining ψ; when (11) and (8) are taken into account, relation (10) goes over into a second-order evolution equation in χ. Together with Eq. (9), these relations make it possible to determine the cross flow field. We note that the initial transverse velocity distribution is completely determined by a single given parameter. As this parameter it is convenient to take the longitudinal vorticity ω, from which it is possible to calculate the initial ψ distribution by solving the equation

$$\operatorname{div}(u\nabla\psi)=-\omega. \tag{12}$$

In the limit of a low degree of nonuniformity of the density field and the longitudinal velocity component, relation (10) goes over into the transfer equation for the longitudinal vorticity. We assume that the nonuniformity of the u distribution over the cross section, equal for the mixing zone to $\delta_u = 1 - m$, and the nonuniformity of ρ, $\delta_p = 1 - n$ are small, i.e., $\delta_u \sim \delta_p \ll 1$ ($m = u_2/u_1$ $n = \rho_2/\rho_1$). Thus,

$$u=u_0(x)(1+\delta_u u_\delta(x,\ y,\ \theta));\ \rho=\rho_0(x)(1+\delta_\rho\rho_\delta(x,\ y,\ \theta)).$$

At the same time, we assume that the vortex component of the transverse velocity V_ω satisfies the condition $\delta_u \ll |V_\omega|/u \ll 1$. If we also take into account the fact that for describing the parameters in the mixing zone the turbulent viscosity coefficient can be assumed to be constant over the cross section [7], up to terms of the order of δ we obtain

$$\partial\omega/\partial x+\operatorname{div}(\mathbf{V}\omega/u_0)=\nu_t\operatorname{div}(\nabla\omega/u_0),$$

which in the approximation in question is equivalent to

$$\frac{\partial}{\partial x}\rho u\left(\frac{\omega}{\rho u}\right)+\operatorname{div}\left(\rho\mathbf{V}\frac{\omega}{\rho u}\right)=\operatorname{div}\left(\rho\nu_t\nabla\frac{\omega}{\rho u}\right). \tag{13}$$

Equations (12) and (13) can be used instead of (10) as an approximate model for calculating the cross flows due to vorticity and in the more general case when the strict limitations on δ are not satisfied. Systematic calculations of the mixing in a cylindrical channel have shown that the approximate model gives good agreement with the results obtained using

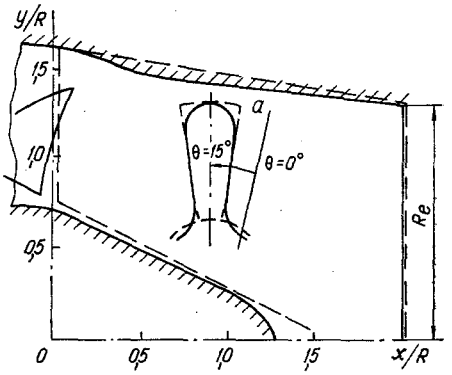

Fig. 1

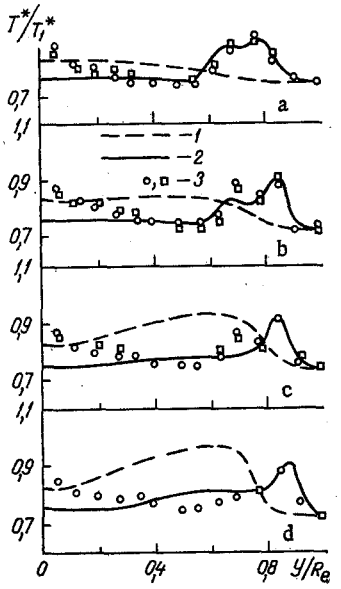

Fig. 2

Fig. 1. Diagram of the mixing exhaust nozzle of a turbofan engine (the broken lines define the calculation domain): a) tab contour at exit face.

Fig. 2. Comparison of calculated and measured stagnation temperature distributions at the nozzle exit: a) $\vartheta = 6°$, b) 9°, c) 12°, d) 15°; 1, 2) calculations without and with allowance for secondary flows respectively; 3) experiment.

the complete equation (10), at least when $m^2n = 1$, $m \geq 0.5$.

3. The system of relations (1), (4), (6), (7), (9), (12), (13) describes weakly expanding flows, i.e., free flows or flows in cylindrical channels. As shown by experience with similar calculations for two-dimensional flows [9], this model can also be used for describing nozzle flow. The approach in question is strictly justified if the nozzle contour $Y_2(x)$ is a slowly varying function, i.e., $dY_2/dx \ll 1$, $d^2Y_2/dx^2 \ll 1$. In fact, however, here too the strong inequalities do not have to be satisfied; nonetheless, it is essential that the nozzle axis be straight.

Our sole aim being to study the mixing process in the nozzle, the boundary layers on the walls were not taken into account. As the boundary conditions we employed the slip and adiabaticity conditions which, on the walls of a nozzle with a slowly varying contour can be represented in the form:

$$\frac{\partial u}{\partial y} = \frac{\partial T^*}{\partial y} = \frac{\partial v_t}{\partial y} = 0, \ \omega = \psi = 0 \text{ when } y = Y_1, \ Y_2,$$
$$\frac{\partial \varphi}{\partial y} = u \frac{dY_1}{dx} \text{ when } y = Y_1, \ \frac{\partial \varphi}{\partial y} = u \frac{dY_2}{dx} \text{ when } y = Y_2, \tag{14}$$

where Y_1 describes the contour of the center body. For numerical integration purposes it is convenient to go over to the new independent variables

$$\xi = x; \ \eta = \frac{y - Y_1(x)}{Y_2(x) - Y_1(x)}. \tag{15}$$

4. Equations (9) and (12) are two-dimensional elliptic equations into which x enters as a parameter, and (1), (4), (7), and (13) are parabolic equations. The parabolic equations are numerically integrated by the longitudinal-transverse method, and the two-dimensional elliptic equations by the iterative longitudinal-transverse method. The computational algorithm as a whole is similar to that used in [6]. However, in our case it was necessary to modify the finite-difference approximation of the convective terms in the parabolic equations. As distinct from [6], where an upstream difference scheme was used, we employed a

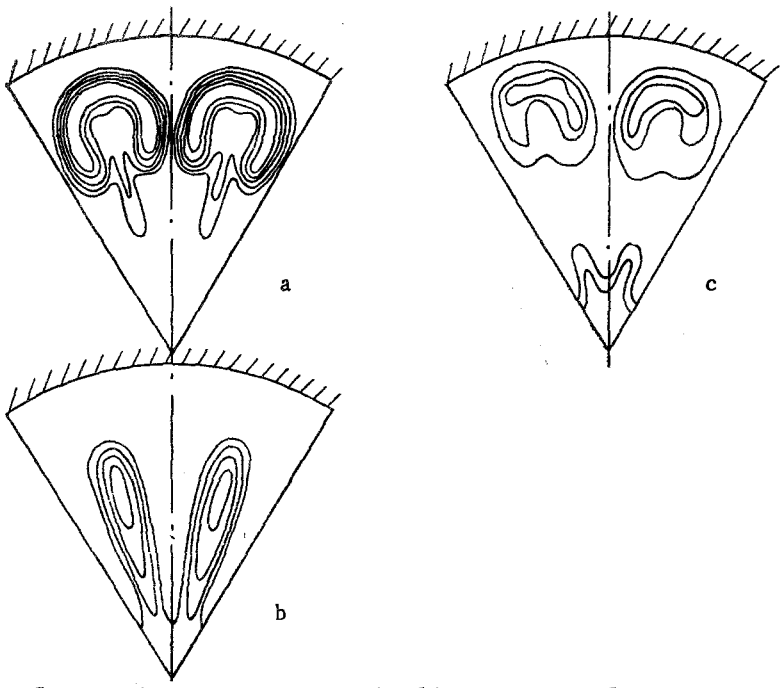

Fig. 3. Stagnation temperature isolines at nozzle exit: a, b) calculations with and without allowance for secondary flows respectively; c) experiment.

second-order-accurate monotonic scheme [10]. As a result of going over to the new scheme we were able considerably to reduce the artificial viscosity which, in an upstream difference scheme with coarse nets in the presence of intense transverse motion in the flow, $|V|/u \sim 0.3$, may exceed the true value of the turbulent viscosity by an order. As the calculations show, the result is a considerable (by up to 30%) overestimation of the mixing intensity.

The calculation method is quite efficient and for the flow through a nozzle typical of modern turbofans (see Fig. 1) makes it possible to obtain a solution in approximately one hour of BÉSM-6 central processor time.

5. To check the possibilities of the calculation method, we examined the operation of a 12-tab mixer mounted in the nozzle shown schematically in Fig. 1. Experimental data on the T^* and V fields in this nozzle were obtained in [1], which also gives the conditions at the mixer exit. The flow is everywhere subsonic, and at the nozzle inlet M = 0.45. The velocity ratio m = 0.861, and from the condition of equality of the total pressures the density ratio $n = 1/m^2$. The u and T^* distributions at the nozzle inlet were assumed to be uniform within each contour. According to the data of [1], the initial value of the turbulent viscosity coefficient can be estimated as $\nu_t/u_1R = 5 \cdot 10^{-4}$. As a result of the flow over the curved surface of the mixer, longitudinal vortices are formed along the lateral edge of the tab (see Fig. 1). In the calculations the ω distribution was assumed to be uniform along the lateral edge, and the intensity of the vortices was taken from the data of [1], where the mean values of the radial velocity in the central sections of the tabs are given. The intensity of the vortex motion may conveniently be characterized by the circulation Γ around a contour embracing half the tab, in other words

$$\Gamma = \int_S \omega dS \tag{16}$$

and for the case in question $\Gamma = -0.34$.

In the cross section the calculation domain is a sector covering half the tab (broken line in Fig. 1). In this section the finite-difference net had 36 × 14 nodes. Since the boundary layer on the walls was not taken into account, it was found expedient to schematize the nozzle contour (broken line in Fig. 1). It should be noted that in the experiments a small separation zone is observed behind the center body; in our calculations, carried out using the parabolized equations, this had to be excluded from consideration.

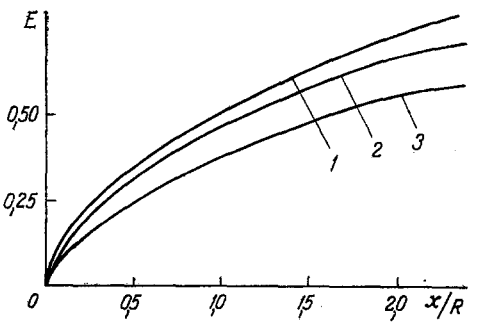

Fig. 4. Extent of mixing as a function of the longitudinal coordinate for various initial secondary flow intensities: 1) $\Gamma = -0.34$, 2) 0.20, 3) 0.

As may be seen from Fig. 2, if the secondary flows at the nozzle inlet are not taken into account (broken curves), then the results are qualitatively quite different. If, however, an initial vorticity is specified in accordance with the experimental data, we get satisfactory quantitative and qualitative agreement in the off-axis hot core zone (continuous curves in Fig. 2). The impossibility of taking into account the boundary layer on the walls of the center body, where there is separation, prevented us from obtaining agreement between the results on the nozzle axis. However, the zone of noncorrespondence of the experimental and calculated data occupies only 4% of the area. An especially clear idea of the action of the secondary flows can be gained from the stagnation temperature isolines in Fig. 3 (in [1] only the qualitative behavior was determined).

Thus, despite the fact that, strictly speaking, the nozzle geometry does not correspond to the concept of a weakly varying contour and the transverse nonuniformity of the parameter fields δ is comparable with the quantity m, the calculation method proposed makes it possible to describe the mixing process downstream of the mixer and determine the flow structure with satisfactory quantitative agreement between the calculated and experimental data.

The effect of flow mixing on the thrust can be characterized by an integral parameter – the extent of mixing [11]. When flows with the same total pressure and a uniform distribution of the parameters at the nozzle inlet are mixed, the extent of mixing E is determined by the nonuniformity of the stagnation temperature field in the outlet section:

$$E = \frac{1 + \frac{S_1 S_2}{(S_1+S_2)^2}\sqrt{\frac{\overline{T_1^*}}{\overline{T_2^*}}}\left(1-\sqrt{\frac{\overline{T_2^*}}{\overline{T_1^*}}}\right)^2 - \frac{1}{S_e^2}\left(\int\limits_{S_e}\sqrt{\overline{T^*}}\,dS\int\limits_{S_e}\frac{dS}{\sqrt{\overline{T^*}}}\right)}{\frac{S_1 S_2}{(S_1+S_2)^2}\sqrt{\frac{\overline{T_1^*}}{\overline{T_2^*}}}\left(1-\sqrt{\frac{\overline{T_2^*}}{\overline{T_1^*}}}\right)^2}. \qquad (17)$$

In Fig. 4 we have plotted the variation of the parameter E along the nozzle channel. With growth in the intensity of the cross flows in the inlet section, the extent of mixing increases by up to 15%, which has a favorable effect on the nozzle thrust characteristics. The reason for this growth is the splitting of the higher-temperature flow into a number of jets (see Fig. 3), with the result that the surface of contact between the hot and cold gases increases.

NOTATION

c_p, specific heat at constant pressure; E, extent of mixing; M, Mach number, m, velocity ratio at the mixer exit; n, density ratio at the mixer exit; P, pressure component constant over the cross section; p, pressure perturbations in the cross section; Pr_t, turbulent Prandtl number; R, radius of a circle with an area equal to the area of the outlet section of the mixer; R_e, radius of the nozzle outlet section; S, cross-sectional area; T^*, stagnation temperature; u, v, and w, components of the velocity vector; V, transverse velocity vector; x, y, and θ, cylindrical coordinates; $Y_1(x)$ and $Y_2(x)$, nozzle contours; Γ, secondary flow circulation; δ, transverse nonuniformity of the parameters; κ, specific heat ratio; ν_t, turbulent viscosity coefficient; ξ, η, and ϑ, transformed coordinates; ρ, density; τ_{yy}, $\tau_{y\theta}$, $\tau_{\theta\theta}$, components of the Reynolds stress tensor; φ, secondary flow potential; ψ, secondary flow stream function; and ω, longitudinal vorticity component. The subscripts 1, 2, and e

relate respectively to the parameters of the inside and outside contours at the mixer exit, and the parameters at the nozzle exit.

LITERATURE CITED

1. B. Anderson, L. Povinelly, and W. Gerstenmaier, "Influence of pressure driven secondary flows on the behavior of turbofan forced mixers," AIAA Paper No. 1198 (1980).
2. S. F. Birch, G. C. Paynter, D. B. Spalding, and D. G. Tatchell, J. Aircr., 15, No. 8, 489-496 (1978).
3. J. P. Kreskovsky, W. R. Briley, and H. McDonald, AIAA J., 22, No. 3, 374-382 (1984).
4. S. V. Patankar and D. B. Spalding, Int. J. Heat Mass Transf., 15, No. 10, 1787-1806 (1972).
5. W. R. Briley and H. McDonald, AIAA Computational Fluid Dynamics Conference July 23-25, 1979, Williamsburg, Va. A collection of technical papers, pp. 74-88.
6. V. I. Vasil'ev and S. Yu. Krasheninnikov, Izv. Akad. Nauk SSSR, Mekh. Zhidk. Gaza, No. 4, 36-44 (1984).
7. G. N. Abramovich, S. Yu. Krasheninnikov, A. N. Sekundov, and I. P. Smirnova, Turbulent Mixing of Gas Jets [in Russian], Moscow (1974).
8. G. N. Abramovich, S. Yu. Krasheninnikov, and A. N. Sekundov, Turbulent Flows in the Presence of Body Forces and Non-Self-Similarity [in Russian], Moscow (1975).
9. A. N. Lanyuk, Izv. Akad. Nauk SSSR, Mekh. Zhidk. Gaza, No. 4, 114-119 (1979).
10. V. P. Kolgan, Uch. Zap. TsAGI, 111, No. 6, 68-77 (1972).
11. V. I. Vasil'ev, S. Yu. Krasheninnikov, and A. D. Portnov, "Jet flows of liquids and gases. Pt. I," Abstr. Proc. All-Union Sci. Conference (2-5 June 1982, Novopolotsk) [in Russian], Novopolotsk Polytech. Inst. (1982), pp. 95-99.

CAUSES OF ENHANCED BOILING HEAT TRANSFER ON SURFACES COVERED WITH PERFORATED POLYMER FILM

V. A. Antonenko

UDC 536.423.1

On the basis of a series of experimental results it is shown that the chief cause of enhanced heat transfer is the concentration of the heat flux in the neighborhood of the perforations.

One of the most efficient methods of enhancing boiling heat transfer in the low-pressure region (below atmospheric) is to cover the heat-transfer surface with perforated polymer film [1, 2].

It is considered [2] that the intensification of heat transfer is achieved mainly as a result of the improved vapor-phase nucleation conditions on the surface of the hydrophobic polymer film. At first glance, this explanation seems quite convincing. However, a careful study of the experimental results [2-10] reveals a very strange fact that cannot be explained from this standpoint. The perforated fluoroplastic (Teflon) film generally employed is, indeed not readily wetted by water ($\Theta > 90°$), however, enhanced heat transfer is also observed in connection with the boiling of other liquids: ethanol [2, 3, 5], the refrigerants R 11, R 12, and R 22 [4, 8, 9], acetone [5], and even helium [10]. All these liquids are good wetters not only of metals but also of fluoroplastics, i.e., for them the latter are not hydrophobic materials. Thus, for example, for fluoroplastic surfaces wetted by ethanol, acetone, and cryogenic fluids $\Theta = 27°$ [11], 25° [12], and not more than 10° [13] respectively.

But what then causes the enhanced heat transfer when hydrophilic perforated film is employed? The model proposed in [2] does not provide an answer to this question.

Institute of Technical Thermophysics, Academy of Sciences of the Ukrainian SSR, Kiev.

Translated from Inzhenerno-Fizicheskii Zhurnal, Vol. 54, No. 4, pp. 573-575, April, 1988. Original article submitted November 27, 1986.